

## RESEARCH ARTICLE

# Role of G protein-coupled receptor 1 in choriocarcinoma progression

Binbin Huang,<sup>1,2\*</sup> Wen Zhu,<sup>1,2\*</sup> Junlei Chang,<sup>3\*</sup> Xiaoyong Dai,<sup>1</sup> Guiyuan Yu,<sup>4</sup> Chen Huang,<sup>1</sup> Esther Wang,<sup>5</sup> Zhihuan Li,<sup>6</sup> Lilong Lin,<sup>6</sup> Baobei Wang,<sup>1</sup> Jie Chen,<sup>1</sup> Tianxia Xiao,<sup>1</sup> Jianmin Niu,<sup>4</sup> and Jian Zhang<sup>1,7</sup>

<sup>1</sup>Center for Reproduction and Health Development, Shenzhen Institutes of Advanced Technology, Chinese Academy of Sciences, Shenzhen, China; <sup>2</sup>Shenzhen College of Advanced Technology, University of Chinese Academy of Sciences, Shenzhen, China; <sup>3</sup>Center for Antibody Drug, Shenzhen Institutes of Advanced Technology, Chinese Academy of Sciences, Shenzhen, China; <sup>4</sup>Shenzhen Maternity and Child Healthcare Hospital, Southern Medical University, Shenzhen, China; <sup>5</sup>Biological Sciences Collegiate Division, University of Chicago, Chicago, Illinois; <sup>6</sup>Dongguan Enlife Stem Cell Biotechnology Institute, Dongguan, China; and <sup>7</sup>Institute for Stem Cell and Regeneration, Chinese Academy of Sciences, Beijing, China

Submitted 20 February 2019; accepted in final form 18 June 2019

Huang B, Zhu W, Chang J, Dai X, Yu G, Huang C, Wang E, Li Z, Lin L, Wang B, Chen J, Xiao T, Niu J, Zhang J. Role of G protein-coupled receptor 1 in choriocarcinoma progression. *Am J Physiol Cell Physiol* 317: C556–C565, 2019. First published June 26, 2019; doi:10.1152/ajpcell.00059.2019.—Choriocarcinoma is characterized by malignant proliferation and transformation of trophoblasts and is currently treated with systemic chemotherapeutic agents. The lack of specific targets for chemotherapeutic agents results in indiscriminate drug distribution. In our study, we aimed to delineate the mechanism by which G protein-coupled receptor 1 (GPR1) regulates the development of choriocarcinoma and thus investigated GPR1 as a prospective chemotherapeutic target. In this study, GPR1 expression levels were examined in several trophoblast cell lines. We found significantly higher GPR1 expression in choriocarcinoma cells (JEG3 and BeWo) than in normal trophoblast cells (HTR-8/SVneo). Additionally, we studied the role of GPR1 in choriocarcinoma in vitro and in vivo. GPR1 knockdown suppressed proliferation, invasion, and Akt and ERK phosphorylation in vitro and slowed tumor growth in vivo. Interestingly, GPR1 overexpression promoted increased proliferation, invasion, and Akt and ERK phosphorylation in vitro. Furthermore, we identified a specific GPR1-binding seven-amino acid peptide, LRH7-G3, that might also suppress choriocarcinoma in vitro and in vivo through phage display. Our study is the first to report that GPR1 may play a role in regulating choriocarcinoma progression through the Akt and ERK pathways. GPR1 could be a promising potential pharmaceutical target for choriocarcinoma.

choriocarcinoma; GPR1; LRH7-G3; phage display

## INTRODUCTION

Choriocarcinoma is the most common epithelial cancer derived from fetal trophoblastic tissues and results from abnormal cellular proliferation of trophoblasts during normal or abnormal pregnancy (27, 29). Choriocarcinoma exhibits malignant growth, widespread metastasis, and abnormal invasion that is distinct from the invasive property of trophoblasts (32). Choriocarcinoma causes morbidity worldwide, affecting two to seven in 100,000 pregnancies in North America and Europe, 5

to 202 in 100,000 pregnancies in Asia, and at an incidence of 5.5% in Africa (2, 9, 32). Currently, chemotherapy is very effective; the survival rate reaches 90% for patients with nonmetastatic choriocarcinoma (3, 14, 27, 32). However, for patients with metastatic choriocarcinoma, complete elimination of cancer cells through chemotherapy treatment proves difficult due to metastasis of choriocarcinoma cells to other organs (except lung tissue). Compounding this problem, patients are very likely to develop chemoresistance after chemotherapy, leading to chemotherapy failures (25, 28). Therefore, it is critical to understand the mechanism of choriocarcinoma development and discover novel pharmaceutical targets for choriocarcinoma.

Chemerin has been shown to bind to its receptors, chemokine-like receptor 1 (CMKLR1), chemokine (C-C motif) receptor-like 2 (CCRL2), and G protein-coupled receptor 1 (GPR1) (5, 39), to play a role in carbohydrate metabolism, adipocyte differentiation, inflammation, and immune responses (4, 26, 30). Recently, a report has indicated that GPR1 can bind to FAM19A1, a new ligand, to regulate proliferation and differentiation in neural stem cells (40). It was previously reported that circulating chemerin was markedly increased in obese patients (8) and gestational diabetes mellitus (GDM) patients, and obesity was positively associated with the risk of GDM in the first trimester (37). In addition, GPR1 is highly expressed in adipose tissue and skeletal muscle. Reports have indicated that GPR1 has a few functions, including a role in glucose homeostasis in obese and pregnant mice (17, 26) and direct or indirect control of progesterone levels by regulating corpus luteum formation (38). With respect to tumors, chemerin promotes squamous cell carcinoma migration via CCRL2 and GPR1, proteins that regulate the MAPK signaling pathway (12). However, the detailed role of GPR1 in choriocarcinoma remains unclear.

The molecular mechanism underlying the carcinogenesis of choriocarcinoma is unclear. Although previous reports found upregulation of some genes and molecules, including metastasis-associated lung adenocarcinoma transcript 1 [MALAT1 (28)], p53, mouse double minute 2 [MDM2 (15)], epidermal growth factor receptor [EGFR (33)], and c-Rel (27), and downregulation of others, including E-cadherin, hypermethylated in cancer 1 protein (HIC-1), tumor suppressor protein

\* B. Huang, W. Zhu, and J. Chang contributed equally to this work.

Address for reprint requests and other correspondence: J. Zhang, Center for Reproduction and Health Development, Shenzhen Institutes of Advanced Technology, Chinese Academy of Sciences, Shenzhen 518055, China (e-mail: jian.zhang@siat.ac.cn).

p16, tissue inhibitor of metalloproteinase-3 [TIMP3 (36)], and microRNA (miR)-519d-3p (10), in choriocarcinoma compared with normal placenta tissue and in choriocarcinoma cell lines compared with normal trophoblast cells (10, 27, 29).

In this study, we investigated GPR1 in choriocarcinoma. We examined the upregulated expression of GPR1 in choriocarcinoma cell lines compared with normal trophoblast cells. Additionally, we established stable transfection of GPR1-knockdown and GPR1-overexpressing choriocarcinoma cell lines to study the role of GPR1 in choriocarcinoma in vitro and in vivo. At present, our results indicate that GPR1 modulates choriocarcinoma cell proliferation and invasion and choriocarcinoma tumor growth via the Akt and ERK pathways.

## MATERIALS AND METHODS

**Cell culture.** JEG3 cells were obtained from the Cell Bank of the Chinese Academy of Sciences (Shanghai, China), BeWo cells were provided by Stanford University (Stanford, CA), HTR-8/SVneo cells were provided by Dr. Charles H. Graham, Queen's University (Kingston, ON, Canada) and cultured in DMEM-F12 (Gibco, Grand Island, NY) supplemented with 10% fetal bovine serum (FBS; Gibco). Cells were cultured as previously described. Stable knockdown and overexpression of GPR1 in JEG3 cells were established using the Lipofectamine 2000 transfection reagent (Invitrogen). The targeted GPR1 short hairpin RNA (shRNA) vector (sense CACTCTCTGATTGT-CATTATAT, anti-sense ATATAATGACAATCAGAGAGTG; Open Biosystems, Shanghai, China) contained a puromycin resistance gene (Invitrogen), and the human GPR1 (NM\_001098199.1) expression vector (Stanford University, Palo Alto, CA) contained a G418 (Geneticin) resistance gene. Transfection with pSM2C-GPR1-shRNA or an empty vector and with pcDNA3.0-GPR1 or an empty vector was carried out according to the manufacturer's protocol, and cells were selected via growth in medium containing 2  $\mu$ g/mL puromycin and 500  $\mu$ g/mL G418 for 2–3 wk. The colonized cells were isolated, amplified, and used for subsequent experiments.

**MTT assay.** The MTT [3-(4,5-dimethylthiazol-2-yl)-2,5-diphenyltetrazolium] assay was used to evaluate cell proliferation and viability. To determine the effect of GPR1 on choriocarcinoma cell proliferation,  $5 \times 10^3$  stably transfected JEG3 cells per well were seeded into 96-well culture plates in DMEM-F12 with 10% FBS at 37°C for 24 h. Then, the proliferation ability of JEG3 cells was measured using MTT at four time points (day 0, 24, 48, and 72 h, Sigma, St. Louis, MO). MTT (20  $\mu$ L, 5 mg/mL) was added to the cells and incubated for 4 h. Then, the medium containing MTT was removed, 150  $\mu$ L of DMSO (Sigma) was added to dissolve the formazan product, and the absorbance was measured as the OD at 490 nm after 30 min.

To study the effect of the specific binding between GPR1 and LRH7-G3 (ChinaPeptides, Shanghai, China) on cell viability,  $5 \times 10^3$  wild-type JEG3 cells/well seeded into 96-well culture plates in DMEM-F12 with 10% FBS at 37°C for 24 h. Then, the cells were starved for 24 h and treated with different concentrations of the GPR1-binding seven-amino acid peptide LRH7-G3 (0, 0.01, 0.1, 1, 10, and 100  $\mu$ M) in the medium with 0.1% FBS for 37°C, and cell viability was measured using the MTT assay at 24 and 48 h.

**Invasion assay.** Cell invasion was studied using Transwell chambers containing Matrigel (24-well inserts; 8  $\mu$ m pore size, 200  $\mu$ g/mL Matrigel, BD Biosciences). Stably transfected choriocarcinoma cells ( $2 \times 10^4$ ) were seeded into the upper chamber in FBS-free medium, and 15% FBS was added to the lower chamber as a chemoattractant. The plates containing chambers were incubated at 37°C in 5% CO<sub>2</sub> for 16 h. Noninvading cells on the surface of the upper chambers were then gently removed. The invading cells on the surface of the lower chambers were fixed in methanol for 10 min, stained with 0.5%

crystal violet for 10 min, and imaged in four randomly selected fields of view using a light microscope.

**Real-time qPCR.** Real-time qPCR was performed as previously described (18, 19). Total RNA was isolated from mouse tissues or cells using RNA plus liquid kits (Takara, Shiga, Japan) following the manufacturer's protocol. RNA (0.5  $\mu$ g) was reverse transcribed into cDNA using reverse transcription kits (Toyobo, Osaka, Japan). The expression levels of several genes were determined by real-time RT-PCR using a Roche LightCycler instrument (Roche, Switzerland) with SYBR Green (Toyobo) detection according to the manufacturer's protocol. Cycle conditions were 30 s at 95°C followed by 45 cycles at 95°C for 5 s, at 60°C for 10 s, and at 72°C for 10 s. *18srRNA* was the housekeeping gene. RT-PCR primers were as follows: human primer sequence of *18srRNA* (NG\_055293: forward CGAAAGC-ATTTGCCAAGAAT, reverse, AGTCGGCATCGTTTATGGTC, PCR production 82 bp; *Gpr1* (XM\_005246471: forward AATGCCA-TCGTCATTGGTT, reverse CAACTGGGCAGTGAAGGAAT, PCR production 192 bp).

**Western blot analysis.** Proteins were extracted from cells. Protein lysates (30–50  $\mu$ g) were added to SDS-PAGE gels and separated at a constant voltage (90 V, 30 min; 120 V, 90 min). Then, proteins were transferred to PVDF membranes at a constant current (250 mA, 2.5 h). Primary antibodies, including  $\beta$ -actin, GPR1, phosphorylated (p)Akt/ Akt (CST, Dallas, TX), pERK/ERK (CST), PCNA, and matrix metalloproteinase-9 (MMP9, CST) antibodies, and horseradish peroxidase (HRP)-conjugated secondary antibody, including anti-mouse and anti-rabbit, were used. The bands were detected using an ECL Western Blot Kit (4A Biotech, Beijing, China).

**Animal experiments and bioluminescence imaging.** Virginal female 8-wk-old BALB/c-null mice were acclimated for 1 wk to their housing conditions: fresh food and water ad libitum, temperature of  $22.0 \pm 1^\circ\text{C}$ , humidity of 40–60% and a 12:12-h light-dark cycle. To determine the effect of GPR1 on choriocarcinoma tumor growth, the mice were randomly divided into two groups. One group of mice was inoculated subcutaneously with  $1 \times 10^6$  JEG3 cells transfected with the luciferase vector (JEG3-luc) and the control vector (scramble) and the other with  $1 \times 10^6$  JEG3-luc cells expressing the shGPR1 vector. The tumor volume was measured and calculated according to the formula ( $\text{mm}^3$ ) =  $1/2 \times \text{length (mm)} \times \text{width (mm)} \times \text{width (mm)}$  every day from day 8 to 17. After 17 days of observation, the mice were euthanized, and tumors were collected. Bioluminescence imaging was performed using an IVIS Spectrum instrument (PerkinElmer) on days 6, 9, and 16. Before imaging, animals were anaesthetized in 2% isoflurane. Luciferin (150 mg/mL, 10  $\mu$ L/10 g body wt (Gold Biotechnology) was injected into the mice 15 min before imaging. After 17 days of observation, the mice were euthanized, and tumors and other organs were collected.

To study the role of LRH7-G3, a specific GPR1-binding seven-amino acid peptide identified by phage display, in choriocarcinoma tumor growth, all mice were inoculated subcutaneously with  $1 \times 10^6$  wild-type JEG-luc cells, and the mice were randomly divided into four groups and injected intraperitoneally with different concentrations of LRH7-G3 (0, 0.3, 3 and 30 mg/kg body wt) daily. The tumor volume was measured. Bioluminescence imaging was performed at weeks 1 and 2 using the IVIS Spectrum instrument (PerkinElmer). After 17 days of observation, the mice were euthanized, and tumors and other organs were collected. All animal experiments were approved by the Committee on the Use of Live Animals for Teaching and Research, Shenzhen Institutes of Advanced Technology, Chinese Academy of Sciences. In addition, all animal experimental methods were conducted in accordance with the approved guidelines and regulations.

**Confocal microscopy.** Colocalization of GPR1 and LRH7-G3 was determined by confocal microscopy as previously described (7). JEG3 cells were incubated with rabbit anti-GPR1 primary antibody to GPR1 (Wuhan Booute Biotechnology, Wuhan, China) and then incubated with goat anti-rabbit IgG Alexa 568 (Invitrogen) and LRH7-G3-FITC (ChinaPeptides).

**Statistical analysis.** All data are presented as means  $\pm$  SE. Statistically significant differences were analyzed using Student's t-test or one-way ANOVA with GraphPad Prism, trial version 7 (GraphPad Software, La Jolla, CA).  $P < 0.05$  was determined to be statistically significant.

## RESULTS

**Expression of GPR1 is significantly upregulated in trophoblastic tumor cell lines.** To determine the effect of GPR1 on trophoblast cells, GPR1 expression levels were first measured by RT-PCR in three trophoblast cell lines. As shown in Fig. 1A, GPR1 expression was significantly upregulated in two choriocarcinoma cell lines, JEG3 and BeWo, in comparison to the normal human trophoblast cell line HTR-8/SVneo. Additionally, Western blotting showed that the translated protein GPR1 was also dramatically increased in the choriocarcinoma cell line (Fig. 1, B and C). These results showed that GPR1 expression was increased in choriocarcinoma cell lines, suggesting its potential involvement in choriocarcinoma progression.

**GPR1 knockdown inhibited Akt and ERK phosphorylation in choriocarcinoma trophoblast cells.** To study GPR1-mediated signal transduction pathways in choriocarcinoma in this study, we first generated stable knockdown and overexpression of GPR1 in choriocarcinoma cell lines. The expression of GPR1 was significantly decreased in the GPR1 knockdown cell line (Fig. 2, A, B, and E, a) and significantly increased in the GPR1-overexpressing cell line (Fig. 2, C, D, and F, a) at both the mRNA and protein levels. Overall, both Akt and ERK phosphorylation showed a positive relationship with GPR1 expression. Loss of GPR1 resulted in a reduction in Akt and ERK phosphorylation in the choriocarcinoma cell line (Fig. 2, B and E, b and c). In contrast, Akt and ERK phosphorylation was visibly increased in the GPR1-overexpressing choriocarcinoma cells (Fig. 2, D and F, b and c). These results indicated that GPR1 could activate both Akt and ERK phosphorylation in choriocarcinoma cells. Additionally, the Western blot results displayed that MMP9, proteins marking invasion, were reduced in GPR1-knockdown cells (Fig. 2, B, and E, d) and increased in GPR1-overexpressing cells (Fig. 2, D and F, d). GPR1 knockdown exhibited reduced PCNA protein expression (Fig. 2, B and E, e), while GPR1 overexpression increased (Fig. 2, D and F, e) PCNA protein expression in choriocarcinoma cells. These results indicate that GPR1 downregulation inhibited the proliferation and invasion of choriocarcinoma

cells at molecular levels, suggestive of the role that GPR1 plays in choriocarcinoma progression.

**GPR1 knockdown inhibited proliferation and invasion of choriocarcinoma cells via Akt and ERK signaling pathways.** To explore the functions of GPR1 in choriocarcinoma cells, we evaluated whether GPR1 affects invasion and proliferation, which are two major characteristics of cancer cells. A transwell assay was then performed to analyze choriocarcinoma cell invasion. Compared with the control (scramble) group, the group with downregulation of GPR1 presented with significantly less invasion of choriocarcinoma cells, as shown in Fig. 3, A and C. Overexpression of GPR1, on the other hand, significantly promoted increased invasion of choriocarcinoma cells compared with that of the empty vector group (Fig. 3, B and D). In addition, the transwell assay and Western blots confirmed that MMP9, proteins marking invasion, were reduced in GPR1-knockdown cells (Fig. 3G) and increased in GPR1-overexpressing cells (Fig. 3H) compared with control choriocarcinoma cells. Cell proliferation was significantly reduced in GPR1-knockdown (Fig. 3E) and increased in GPR1-overexpressing (Fig. 3F) choriocarcinoma cells in the MTT assay. Additionally, the Western blot results for the proliferation-related protein PCNA were also consistent with the MTT assay. GPR1 knockdown exhibited reduced PCNA protein expression (Fig. 3G), whereas GPR1 overexpression increased (Fig. 3H) PCNA protein expression in choriocarcinoma cells. These results indicate that GPR1 downregulation inhibited the proliferation and invasion of choriocarcinoma cells at the phenotypic level.

It has previously been reported that Akt and ERK play a role in trophoblastic tumor cells (34). In this study, we have proven that GPR1 regulates Akt and ERK phosphorylation (Fig. 2). Thus, we hypothesized that GPR1 may regulate choriocarcinoma progression through the Akt and ERK pathways. To further corroborate these results, cells were pretreated with selective inhibitors of both signaling pathways under conditions of GPR1 knockdown and overexpression. Inhibition of PI3K kinase by wortmannin (Wor) resulted in reduced Akt phosphorylation (Fig. 3G). The regulation of MMP9 by GPR1 (Fig. 2) was evaluated. The results indicated that MMP9 was decreased in GPR1-knockdown choriocarcinoma cells treated with Wor; U0126, an inhibitor of ERK phosphorylation, reduced ERK phosphorylation (Fig. 3H). Interestingly, U0126 reduced MMP9 phosphorylation in choriocarcinoma cells. Combining this information with the results shown in Figs. 2

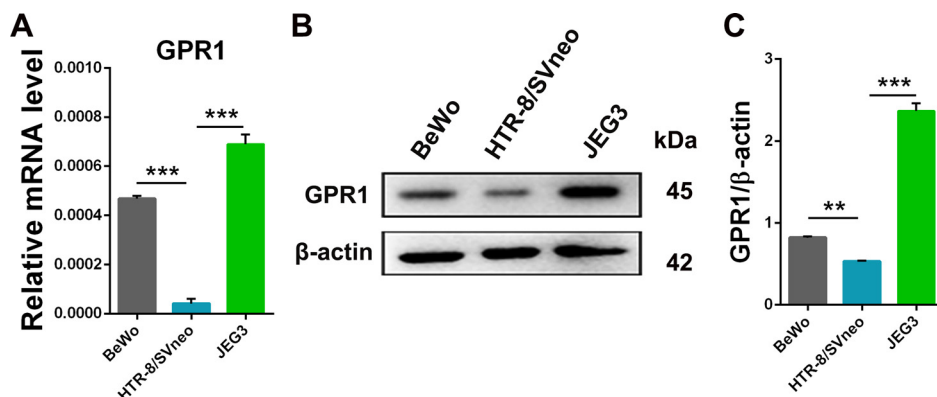


Fig. 1. Expression of G protein-coupled receptor 1 (GPR1) in trophoblast cell lines. A and B: quantitative real-time PCR analysis of GPR1 mRNA expression (A) and Western blotting analysis of GPR1 protein expression (B) in a normal trophoblast cell line (HTR8/SVneo) and trophoblastic tumor cell lines BeWo and JEG3. C: quantification of GPR1 protein from B. Three independent experiments were performed. Results are expressed as means  $\pm$  SE.  $**P < 0.01$ ,  $***P < 0.001$ .



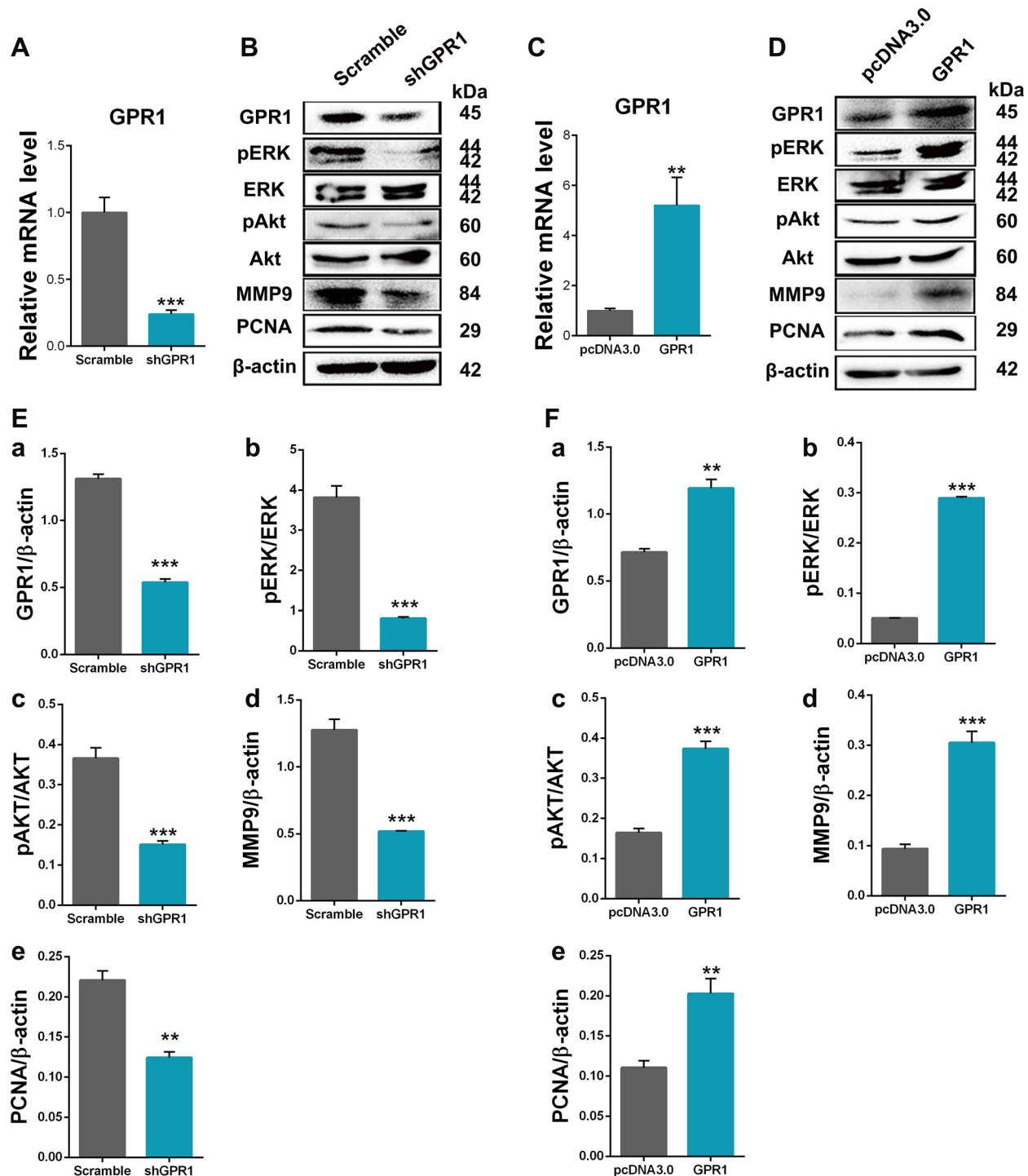


Fig. 2. G protein-coupled receptor 1 (GPR1) regulates Akt and ERK signaling pathways in choriocarcinoma trophoblast cell line JEG3. *A* and *C*: quantitative real-time PCR analysis of GPR1 mRNA expression in choriocarcinoma cells with GPR1 knockdown (*A*) and GPR1 overexpression (*C*). *B* and *D*: Western blotting analysis of GPR1, ERK/phosphorylated (p)ERK, and Akt/pAkt protein expression in choriocarcinoma cells with GPR1 knockdown (*B*) and GPR1 overexpression line (*D*). MMP9, matrix metalloproteinase-9. *E*, *a–e*: quantification of protein expression from *B*. *F*, *a–e*: quantification of protein expression from *D*. Three independent experiments were performed. Results are expressed as means  $\pm$  SE. \*\* $P$  < 0.01, \*\*\* $P$  < 0.001.

and 3 indicated that GPR1 knockdown suppressed the invasion and expression of matrix metalloproteinases (MMPs) (Fig. 3, *C*, *E*, and *G*). These results suggest that GPR1's role in invasion involves its regulation of invasion-related proteins through the ERK pathway but not the Akt pathway. MTT assays were used to evaluate the effect of the Akt and ERK

pathways on proliferation. The results showed that decreased Akt phosphorylation resulted in a decrease in the proliferation rate. As shown in Fig. 3, *E* and *I*, the proliferation rate was significantly decreased both in GPR1-knockdown choriocarcinoma cells compared with control (scramble) cells and in control (scramble) choriocarcinoma

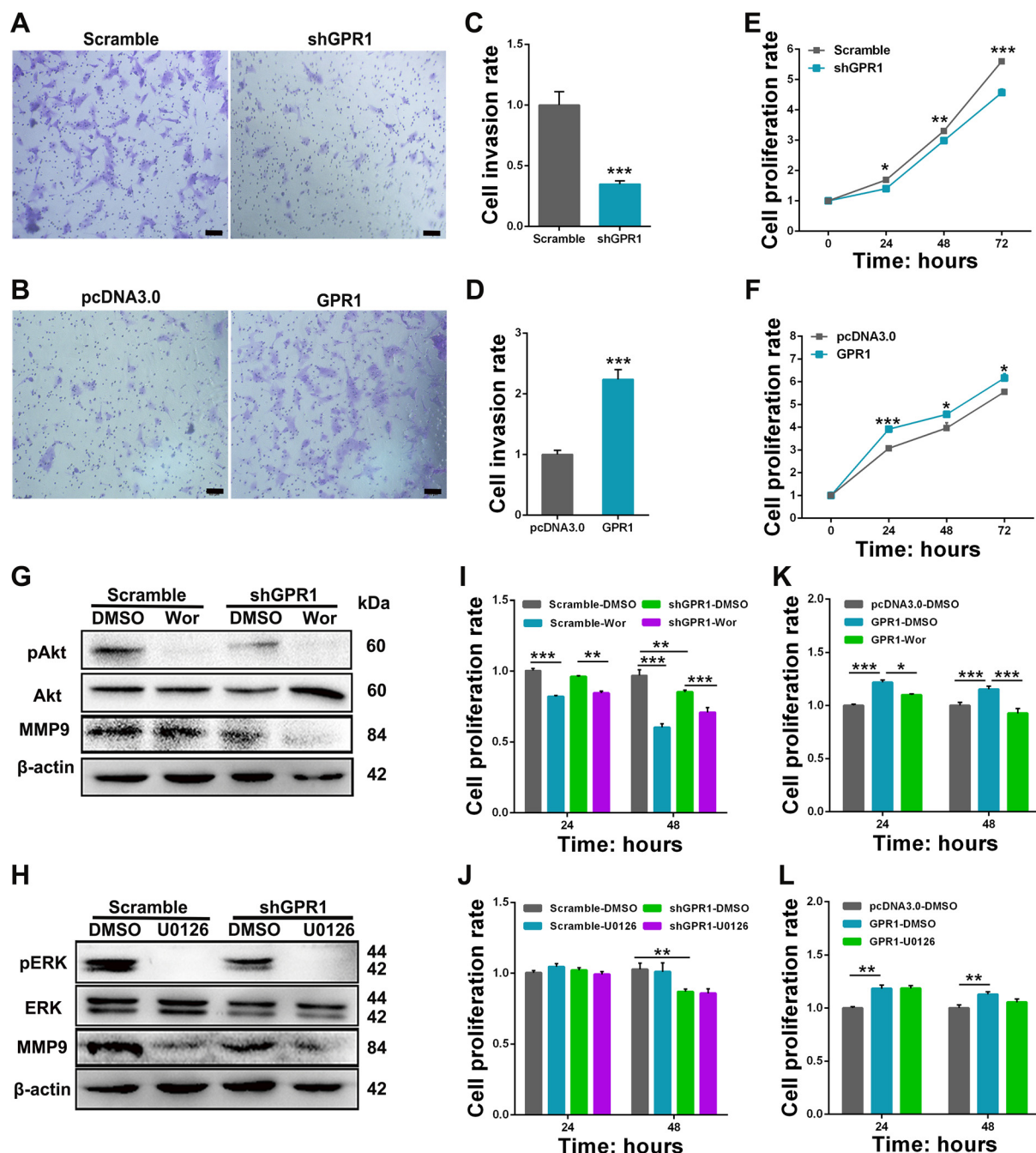


Fig. 3. G protein-coupled receptor 1 (GPR1) regulated proliferation and invasion of choriocarcinoma cells. Invasion ability was analyzed in choriocarcinoma cells with GPR1 knockdown (A) and GPR1 overexpression (B) by transwell assay, including quantitative results (C and D) corresponding to A and B, MTT assay analysis of proliferation in choriocarcinoma cells with GPR1 knockdown (E) and GPR1 overexpression line (F), respectively. Western blotting analysis of expression of phosphorylated (p)Akt/Akt, pERK/ERK, and the invasion-related protein matrix metalloproteinase-9 (MMP9) in choriocarcinoma cells with GPR1 knockdown that were treated with a pAkt inhibitor [wortmannin (Wor); G] and a pERK inhibitor (U0126; H). MTT assay analysis of proliferation in the GPR1-knockdown choriocarcinoma cells treated with a pAkt inhibitor (Wor; I) and a pERK inhibitor (U0126; J) and in the GPR1-overexpressing choriocarcinoma cells treated with a pAkt inhibitor (Wor; K) and a pERK inhibitor (U0126; L). Three independent experiments were performed. Results are expressed as means  $\pm$  SE. \* $P$  < 0.05, \*\* $P$  < 0.01, \*\*\* $P$  < 0.001.

cells treated with Wor compared with control cells treated with DMSO for 24 h. The proliferation rate was significantly decreased in both scramble and GPR1-knockdown choriocarcinoma cells treated with Wor compared with corresponding cells treated with DMSO for 48 h. Overall, proliferation was significantly increased in GPR1-overexpressing cells compared with empty vector-transfected cho-

riocarcinoma cells (Fig. 3F). Inhibition of Akt phosphorylation limited the proliferation of GPR1-overexpressing choriocarcinoma cells treated with Wor compared with that of cells treated with DMSO for the 24- and 48-h time points (Fig. 3K). However, significant differences in proliferation were not observed in treatments with U0126, an inhibitor of ERK phosphorylation (Fig. 3, J and L). These results indi-

cated that GPR1 regulated proliferation via the Akt signaling pathway but not ERK in choriocarcinoma cells.

**GPR1 knockdown suppressed choriocarcinoma tumor growth.** To investigate whether GPR1 plays a role in choriocarcinoma, tumor models were generated by subcutaneous inoculation of either JEG3-luc cells expressing the control vector (scramble) or  $1 \times 10^6$  JEG3-luc cells expressing the shGPR1 vector. Tumor volumes and weights were measured. The tumor volumes (Fig. 4, A and B) and weights (Fig. 4D) were significantly decreased after GPR1 knockdown. GPR1 knockdown suppressed choriocarcinoma tumor growth (Fig. 4, C and E); this result was further confirmed using in vivo imaging at 6, 9, and 16 days after injection. Quantification of the results in mice showed that GPR1 knockdown decreased the intensity of the quantified region of interest (ROI) and that there was a statistically significant difference at day 16, as shown in Fig. 4F. These results indicated that the knockdown of GPR1 could slow the tumor growth of choriocarcinoma in a mouse model.

**LRH7-G3, a specific GPR1-binding peptide, suppressed choriocarcinoma tumor growth.** The results above indicate that GPR1 is involved in regulating choriocarcinoma progression in

vitro and in vivo. We also explored the potential of GPR1 as a pharmaceutical target for choriocarcinoma. LRH7-G3, a specific seven-amino acid peptide binding to GPR1, was identified via phage display technology by our laboratory (7). Confocal microscopy was performed to observe the specific binding of LRH7-G3 to GPR1 in choriocarcinoma cells. As shown in Fig. 5A, the GPR1 staining (red) was stronger in the choriocarcinoma cells than in the similar cells with GPR1 knockdown. In addition, GPR1 and LRH7-G3 (FITC) were colocalized in the choriocarcinoma cells, and the LRH7-G3 staining (green) was consistent with the GPR1 staining in choriocarcinoma cells. Then, MTT assays were used to evaluate the proliferation ability of choriocarcinoma cells treated with the different concentrations of LRH-G3 (0, 0.01, 0.1, 1, 10, and 100  $\mu$ M). Choriocarcinoma cells treated with the highest concentration (100  $\mu$ M) displayed significantly lower rates of proliferation compared with cells treated with the lower concentrations of LRH-G3 for 24 and 48 h (Fig. 5B). In addition, LRH7-G3 could also inhibit Akt/pAkt (Fig. 5, C–G) and ERK/pERK, PCNA, and MMP9 protein in wild-type JEG3 cells, which were consistent with in GPR1-knockdown JEG3. These data suggest that LRH7-G3 may specifically bind to GPR1 and

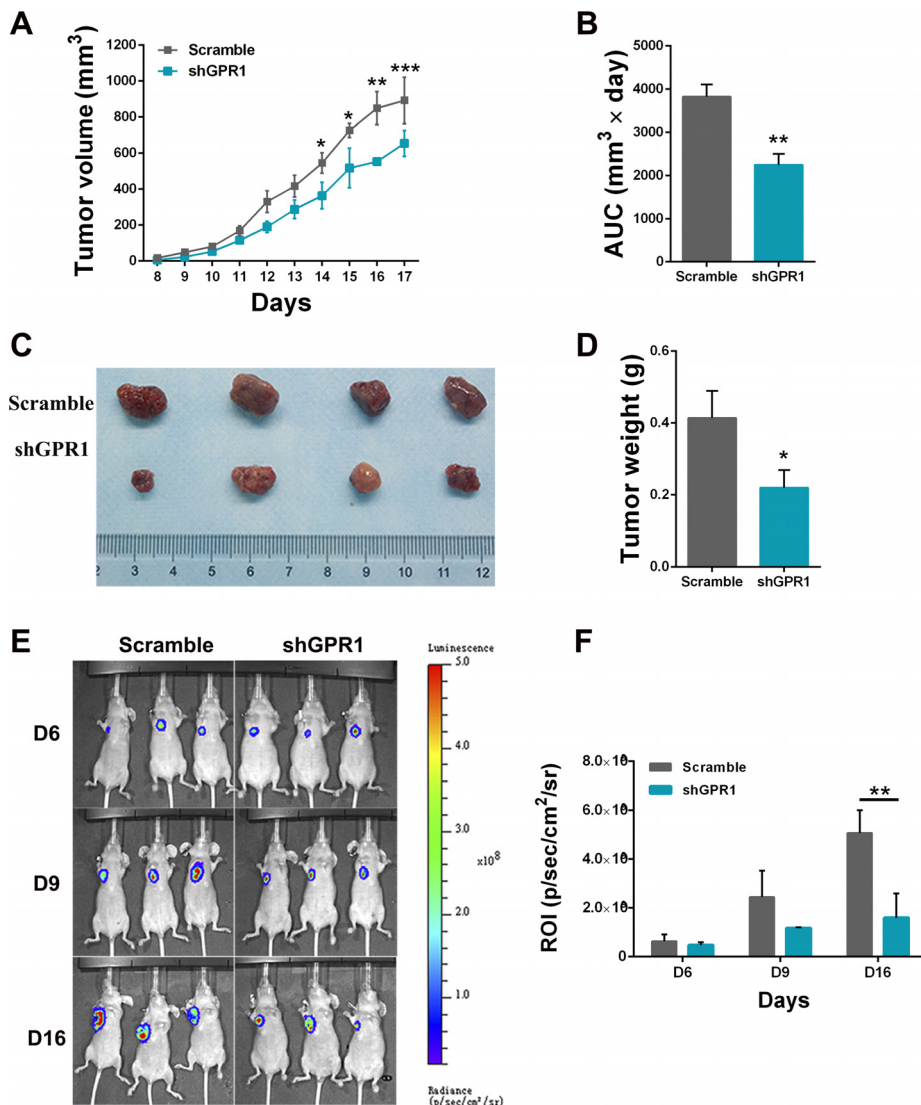


Fig. 4. G protein-coupled receptor 1 (GPR1)-related choriocarcinoma tumor growth. A and B: tumor volumes were measured (A) and area under the curve (AUC; B) was calculated from A. C: representative images of the whole resected tumor are shown. D: tumor weight was measured at day 16. E: tumor sites were evaluated via in vivo images of mice with an IVIS Spectrum optical imaging system. F: fluorescence signals of tumors were quantitated from E. ROI, region of interest. Results are expressed as means  $\pm$  SE. \* $P$  < 0.05, \*\* $P$  < 0.01, \*\*\* $P$  < 0.001.



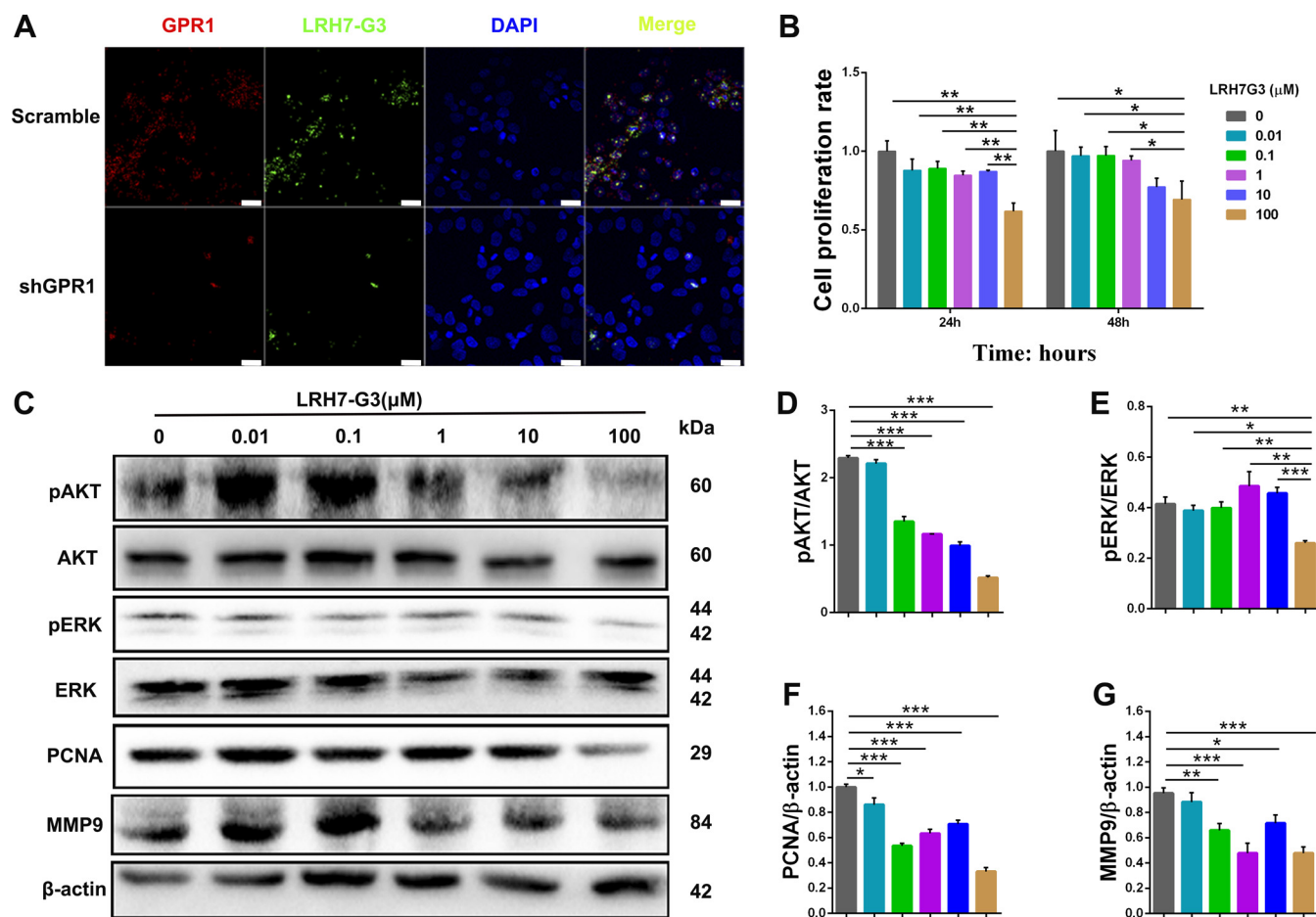


Fig. 5. LRH7-G3, a specific G protein-coupled receptor 1 (GPR1)-binding peptide, suppressed choriocarcinoma cell proliferation. **A**: colocalization of LRH7-G3 (FITC-LRH7-G3) with GPR1 (red) in GPR1-knockdown choriocarcinoma cells. **B**: MTT assay analysis of proliferation in choriocarcinoma cells treated with different concentrations of LRH7-G3. **C**: Western blotting analysis of Akt/phosphorylated (p)Akt and ERK/pERK, PCNA, and matrix metalloproteinase-9 (MMP9) protein expression in JEG3 treatment with different concentrations of LRH7-G3. **D–G**: quantification of protein expression from **C**. Three independent experiments were performed. Results are expressed as means  $\pm$  SE. \* $P$  < 0.05, \*\* $P$  < 0.01, and \*\*\* $P$  < 0.001.

subsequently limit choriocarcinoma cell proliferation through GPR1 signaling. Additionally, animal experiments were performed to obtain further evidence proving the suitability of GPR1 as a pharmaceutical target for choriocarcinoma. Tumor models were generated by subcutaneous inoculation of  $1 \times 10^6$  JEG3-luc cells treated with concentrations of LRH7-G3 (0, 0.3, 3, and 30 mg/kg) by intraperitoneal injection daily. Tumor volumes were measured, and the volumes were quantified according to the areas under the curve (AUCs). As shown in Fig. 6, **A** and **B**, compared with the control, groups treated with LRH7-G3 presented with significantly decreased choriocarcinoma tumor growth. The tumors in these groups also appeared to shrink compared with those of the controls, as found in the mice that were euthanized 17 days after injection (Fig. 6C). Tumor weights were also significantly decreased in the mice treated with the different concentrations of LRH7-G3 compared with the control mice (Fig. 6E), which was also confirmed by in vivo imaging. Quantification of mice showed that GPR1 knockdown decreased the intensity of the quantified ROI by a statistically significant difference (Fig. 6F). Additionally, tumor and kidney morphologies in groups treated with different concentrations of LRH7-G3 were analyzed by hematoxylin and eosin (HE) staining. Apoptosis was identified

according to recently recommended morphological features (11, 21). Apoptotic cells with cytoplasmic and nuclear condensation and nuclear fragmentation (arrows) were observed in the LRH7-G3 groups (Fig. 6G). A drug toxicity test was performed by evaluating the kidney. According to HE staining, compared with the controls, LRH7-G3 did not significantly alter the morphology of the glomeruli (Fig. 6G). These results indicated that LRH7-G3, a specific GPR1-binding peptide, suppressed choriocarcinoma progression and that GPR1 may be a potential pharmaceutical target for choriocarcinoma.

## DISCUSSION

In this study, we evaluated the expression of GPR1 in several trophoblastic cells, including normal and choriocarcinoma cell lines, due to the lack of clinical samples. We first found choriocarcinoma cell lines, BeWo and JEG3, that expressed higher levels of GPR1 than that of a normal cell line, HTR8/SVneo. BeWo and JEG3 are derived from choriocarcinoma, and HTR8/SVneo was developed from first trimester extravillous trophoblasts infected with simian virus 40 large T antigen (1, 13, 16). We found that loss of GPR1 function resulted in suppressed choriocarcinoma cell proliferation in vitro

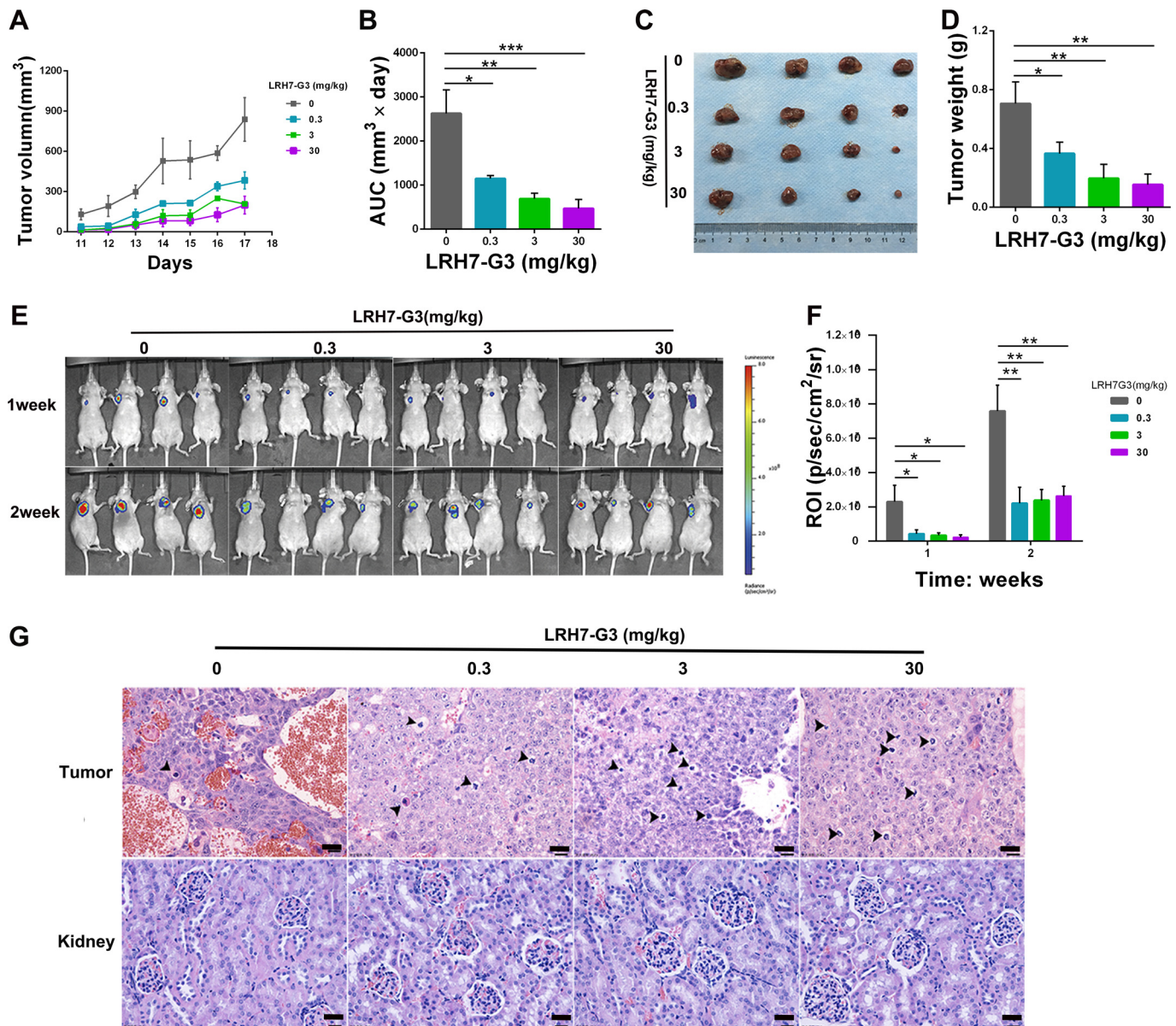


Fig. 6. Specific G protein-coupled receptor 1 (GPR1)-binding LRH7-G3 inhibited choriocarcinoma tumor growth in vivo. *A* and *B*: tumor volumes were measured (*A*) and the area under the curve (AUC; *B*) was calculated from *A*. *C*: representative images of whole resected tumors are shown. *D*: tumor weights were measured during treatment with different concentrations of LRH7-G3. *E*: tumor sites were evaluated via in vivo images of mice with an IVIS Spectrum optical imaging system. *F*: fluorescence signals of tumors were quantitated from *E*. ROI, region of interest. *G*: hematoxylin and eosin (HE) staining analysis of tumor and kidney morphology (black arrows indicate apoptotic cells). Results are expressed as means  $\pm$  SE. \**P* < 0.05, \*\**P* < 0.01, and \*\*\**P* < 0.001.

and in vivo, decreased invasion in these lines, and decreased Akt and ERK pathway phosphorylation. Our study provides the first evidence for a mechanism by which GPR1 regulates choriocarcinoma progression.

In a previous study, GPR1 was detected in adipose tissue, muscle, pancreas, and neural stem cells (30). Additionally, it has been reported that GPR1 plays a role in lipid metabolism (20), glucose homeostasis (26), and stem cell differentiation and proliferation (40). However, GPR1 has not previously been shown to play a role in trophoblast physiology. Although chemotherapy provides high cure rates for most patients with choriocarcinoma, patients are very likely to develop chemoresistance after chemotherapy, leading to chemotherapy failures.

Hence, it is urgent that novel pharmaceutical targets for choriocarcinoma are found and developed for use.

First, our experiments showed that proliferation was significantly decreased in GPR1-knockdown JEG3 cells and increased in GPR1-overexpressing JEG3 cells. Western blotting analysis showed a PCNA decrease in GPR1-knockdown cells and a PCNA increase in GPR1-overexpressing cells. PCNA is a cell proliferation marker; it is present only during active phases of the cell cycle (6) and is a member of the DNA sliding clamp family of proteins involved in DNA replication and repair. PCNA can also form complexes with cyclin-CDK complexes, whose phosphorylation is stimulated, leading to control of cell cycle progression (23). As shown by our results,



choriocarcinoma cell line proliferation may be regulated by the Akt pathway (32, 34). Akt phosphorylation was downregulated in GPR1-knockdown JEG3 cells and upregulated in GPR1-overexpressing JEG3 cells. Further supporting our results, it has previously been reported that GPR1 could be involved in progesterone secretion through the phosphoinositide 3-kinase (PI3K)-Akt pathway (38). Additionally, in GPR1-overexpressing JEG3 cells, we observed a reduction in proliferation after treatment with a PI3K inhibitor. This result demonstrates that GPR1 regulates choriocarcinoma cell proliferation through the PI3K-Akt pathway.

Second, GPR1 is a key factor in choriocarcinoma cells and a strong activator of their invasion. Invasion was significantly suppressed by GPR1 knockdown and promoted by GPR1 overexpression in JEG3 cells. We not only found that both Akt and ERK phosphorylation were different in stably transfected JEG3 cells, but we also showed that GPR1 regulates invasion and invasion-related molecules, including MMP9. According to previous studies, the ERK pathway is regarded as the main signaling pathway involved in breast cancer (24). Collectively, we observed a reduction in MMP9 in stably transfected JEG3 cells treated with the ERK1/2 inhibitor U0126. Therefore, our results indicate that GPR1 regulates choriocarcinoma cell invasion through the ERK pathway. The gelatinase MMP9 is expressed on trophoblast cells and has already been reported to be a key enzyme in the choriocarcinoma invasion process (35).

Additionally, we also showed that tumor growth was slowed after reducing GPR1 in vivo by a tumorigenesis model. These results indicate that GPR1 may be a potential pharmaceutical target for choriocarcinoma. Therefore, we used phage display to identify a peptide that specifically binds to GPR1 to treat choriocarcinoma tumors in vivo by phage display, as previously described (22). In our study, we used a phage-displayed heptapeptide library to identify GPR1 antagonists, and we successfully isolated the seven-amino acid peptide named LRH7-G3. Thus far, we have not found any related antagonists for GPR1. Choriocarcinoma tumorigenesis showed that LRH7-G3 had high effectiveness in suppressing tumor growth. At present, there are some reports showing that some molecules and genes, including MALAT1, p53, MDM2, EGFR, and c-Rel or E-cadherin, HIC-1, p16, TIMP3, and MiR-519d-3p, affect choriocarcinoma progression. However, these studies remain in the laboratory stage and we did not use tools to isolate drugs or chemical reagents as treatment targets. Although we evaluated cells with GPR1 downregulation and knockdown in our study, we have no clinical samples to confirm whether GPR1 is highly expressed in choriocarcinoma.

In summary, our findings support our hypothesis that GPR1 is a key regulator for choriocarcinoma. However, future studies will be needed to further this investigation on GPR1 signaling. In conclusion, we have successfully identified an antagonist that is highly effective in treating tumors in vivo. Therefore, our study has discerned a promising potential pharmaceutical target for treating choriocarcinoma in a safer and less toxic manner than multiagent chemotherapies. The GPR1 antagonist LRH7-G3 was identified to have an effect in a variety of cancers characterized by the upregulation of GPR1.

#### ACKNOWLEDGMENTS

Correspondence may also be addressed to J. Niu (njianmin@163.com).

#### GRANTS

This study was supported by the National Key Research and Development Program of China (2018YFC1003703), by the Strategic Priority Research Program of the Chinese Academy of Sciences, Grant No. XDA16020702, the National Natural Science Foundation of China (81830041), Shenzhen grants (KQJSCX2017033116131058, JCYJ20170817143406822, JCYJ2017030717-0338498, and JCYJ20170818154558312), the SIAT-ZKFB Joint Laboratory for Cell Technology Development and Application and the SIAT-GHMSCB Biomedical Laboratory for Major Diseases, Guangdong Innovation Platform of Translational Research for Cerebrovascular Diseases and Guangdong Key Laboratory of Nanomedicine.

#### DISCLOSURES

No conflicts of interest, financial or otherwise, are declared by the authors.

#### AUTHOR CONTRIBUTIONS

J.N. and J.Z. conceived and designed research; B.H., W.Z., J. Chang, X.D., G.Y., C.H., E.W., Z.L., L.L., B.W., J. Chen, and T.X. performed experiments; B.H., J. Chang, and J.Z. analyzed data; B.H. interpreted results of experiments; B.H. prepared figures; B.H. and W.Z. drafted manuscript; B.H., J. Chang, E.W., Z.L., L.L., J. Chen, T.X., J.N., and J.Z. edited and revised manuscript; B.H., W.Z., J. Chang, X.D., G.Y., C.H., E.W., Z.L., L.L., B.W., J. Chen, T.X., J.N., and J.Z. approved final version of manuscript.

#### REFERENCES

1. Abou-Kheir W, Barrak J, Hadadeh O, Daoud G. HTR-8/SVneo cell line contains a mixed population of cells. *Placenta* 50: 1–7, 2017. doi:10.1016/j.placenta.2016.12.007.
2. Altieri A, Franceschi S, Ferlay J, Smith J, La Vecchia C. Epidemiology and aetiology of gestational trophoblastic diseases. *Lancet Oncol* 4: 670–678, 2003. doi:10.1016/S1470-2045(03)01245-2.
3. Bagley RG, Ren Y, Kurtzberg L, Weber W, Bangari D, Brondyk W, Teicher BA. Human choriocarcinomas: placental growth factor-dependent preclinical tumor models. *Int J Oncol* 40: 479–486, 2012. doi:10.3892/ijo.2011.1257.
4. Banas M, Zegar A, Kwitniewski M, Zabieglo K, Marczyńska J, Kapinska-Mrowiecka M, Lajevic M, Zabel BA, Cichy J. The expression and regulation of chemerin in the epidermis. *PLoS One* 10: e0117830, 2015. doi:10.1371/journal.pone.0117830.
5. Barnea G, Strapps W, Herrada G, Berman Y, Ong J, Kloss B, Axel R, Lee KJ. The genetic design of signaling cascades to record receptor activation. *Proc Natl Acad Sci USA* 105: 64–69, 2008. doi:10.1073/pnas.0710487105.
6. Bologna-Molina R, Mosqueda-Taylor A, Molina-Frechero N, Mori-Estevez AD, Sánchez-Acuña G. Comparison of the value of PCNA and Ki-67 as markers of cell proliferation in ameloblastic tumors. *Med Oral Patol Oral Cir Bucal* 18: e174–e179, 2013. doi:10.4317/medoral.18573.
7. Cai C, Dai X, Zhu Y, Lian M, Xiao F, Dong F, Zhang Q, Huang Y, Zheng Q. A specific RAGE-binding peptide biopanning from phage display random peptide library that ameliorates symptoms in amyloid  $\beta$  peptide-mediated neuronal disorder. *Appl Microbiol Biotechnol* 100: 825–835, 2016. doi:10.1007/s00253-015-7001-7.
8. Chang SS, Eisenberg D, Zhao L, Adams C, Leib R, Morser J, Leung L. Chemerin activation in human obesity. *Obesity (Silver Spring)* 24: 1522–1529, 2016. doi:10.1002/oby.21534.
9. Cisse CT, Lo N, Moreau JC, Fall-Gaye C, Mendez V, Diadhiou F. [Choriocarcinoma in Senegal: epidemiology, prognosis and prevention]. *Gynécol Obstét Fertil* 30: 862–869, 2002. doi:10.1016/S1297-9589(02)00456-3.
10. Ding J, Huang F, Wu G, Han T, Xu F, Weng D, Wu C, Zhang X, Yao Y, Zhu X. MiR-519d-3p suppresses invasion and migration of trophoblast cells via targeting MMP-2. *PLoS One* 10: e0120321, 2015. doi:10.1371/journal.pone.0120321.
11. Elmore SA, Dixon D, Hailey JR, Harada T, Herbert RA, Maronpot RR, Nolte T, Rehg JE, Rittinghausen S, Rosol TJ, Satoh H, Vidal JD, Willard-Mack CL, Creasy DM. Recommendations from the INHAND Apoptosis/Necrosis Working Group. *Toxicol Pathol* 44: 173–188, 2016. doi:10.1177/0192623315625859.
12. Farsam V, Basu A, Gatzka M, Treiber N, Schneider LA, Mulaw MA, Lucas T, Kochanek S, Dummer R, Levesque MP, Wlaschek M, Scharffetter-Kochanek K. Senescent fibroblast-derived Chemerin pro-

- motes squamous cell carcinoma migration. *Oncotarget* 7: 83554–83569, 2016. doi:10.18632/oncotarget.13446.
13. Ferretti C, Bruni L, Dangles-Marie V, Pecking AP, Bellet D. Molecular circuits shared by placental and cancer cells, and their implications in the proliferative, invasive and migratory capacities of trophoblasts. *Hum Reprod Update* 13: 121–141, 2007. doi:10.1093/humupd/dml048.
  14. Foulmann K, Guastalla JP, Caminet N, Trillet-Lenoir V, Raudrant D, Gollfier F, Schott AM. What is the best protocol of single-agent methotrexate chemotherapy in nonmetastatic or low-risk metastatic gestational trophoblastic tumors? A review of the evidence. *Gynecol Oncol* 102: 103–110, 2006. doi:10.1016/j.ygyno.2006.02.038.
  15. Fulop V, Mok SC, Genest DR, Gati I, Doszpod J, Berkowitz RS. p53, p21, Rb and mdm2 oncoproteins. Expression in normal placenta, partial and complete mole, and choriocarcinoma. *J Reprod Med* 43: 119–127, 1998.
  16. Hannan NJ, Paiva P, Dimitriadis E, Salamonsen LA. Models for study of human embryo implantation: choice of cell lines? *Biol Reprod* 82: 235–245, 2010. doi:10.1095/biolreprod.109.077800.
  17. Huang B, Huang C, Zhao H, Zhu W, Wang B, Wang H, Chen J, Xiao T, Niu J, Zhang J. Impact of GPR1 signaling on maternal high-fat feeding and placenta metabolism in mice. *Am J Physiol Endocrinol Metab* 316: E987–E997, 2019. doi:10.1152/ajpendo.00437.2018.
  18. Huang BB, Liu XC, Qin XY, Chen J, Ren PG, Deng WF, Zhang J. Effect of high-fat diet on immature female mice and messenger and noncoding RNA expression profiling in ovary and white adipose tissue. *Reprod Sci* 1933719118765966, 2018. doi:10.1177/1933719118765966.
  19. Huang C, Huang BB, Niu JM, Yu Y, Qin XY, Yang YL, Xiao TX, Chen J, Ren LR, Zhang JV. Global mRNA and long non-coding RNA expression in the placenta and white adipose tissue of mice fed a high-fat diet during pregnancy. *Cell Physiol Biochem* 50: 2260–2271, 2018. doi:10.1159/000495086.
  20. Huang J, Zhang J, Lei T, Chen X, Zhang Y, Zhou L, Yu A, Chen Z, Zhou R, Yang Z. Cloning of porcine chemerin, ChemR23 and GPR1 and their involvement in regulation of lipogenesis. *BMB Rep* 43: 491–498, 2010. doi:10.5483/BMBRep.2010.43.7.491.
  21. Jivan R, Peres J, Damelin LH, Wade R, Veale RB, Prince S, Mavri-Damelin D. Disulfiram with or without metformin inhibits oesophageal squamous cell carcinoma in vivo. *Cancer Lett* 417: 1–10, 2018. doi:10.1016/j.canlet.2017.12.026.
  22. Kang J, Zhao G, Lin T, Tang S, Xu G, Hu S, Bi Q, Guo C, Sun L, Han S, Xu Q, Nie Y, Wang B, Liang S, Ding J, Wu K. A peptide derived from phage display library exhibits anti-tumor activity by targeting GRP78 in gastric cancer multidrug resistance cells. *Cancer Lett* 339: 247–259, 2013. doi:10.1016/j.canlet.2013.06.016.
  23. Koundrioukoff S, Jónsson ZO, Hasan S, de Jong RN, van der Vliet PC, Hottiger MO, Hübscher U. A direct interaction between proliferating cell nuclear antigen (PCNA) and Cdk2 targets PCNA-interacting proteins for phosphorylation. *J Biol Chem* 275: 22882–22887, 2000. doi:10.1074/jbc.M001850200.
  24. Lee JH, Jung SM, Yang KM, Bae E, Ahn SG, Park JS, Seo D, Kim M, Ha J, Lee J, Kim JH, Kim JH, Ooshima A, Park J, Shin D, Lee YS, Lee S, van Loo G, Jeong J, Kim SJ, Park SH. A20 promotes metastasis of aggressive basal-like breast cancers through multi-monoubiquitylation of Snail1. *Nat Cell Biol* 19: 1260–1273, 2017. doi:10.1038/ncb3609.
  25. Lurain JR, Singh DK, Schink JC. Primary treatment of metastatic high-risk gestational trophoblastic neoplasia with EMA-CO chemotherapy. *J Reprod Med* 51: 767–772, 2006.
  26. Rourke JL, Muruganandan S, Dranse HJ, McMullen NM, Sinal CJ. Gpr1 is an active chemerin receptor influencing glucose homeostasis in obese mice. *J Endocrinol* 222: 201–215, 2014. doi:10.1530/JOE-14-0069.
  27. Sekiya Y, Yamamoto E, Niimi K, Nishino K, Nakamura K, Kotani T, Kajiyama H, Shibata K, Kikkawa F. c-Rel promotes invasion of choriocarcinoma cells via PI3K/AKT signaling. *Oncology* 92: 299–310, 2017. doi:10.1159/000458529.
  28. Shi D, Zhang Y, Lu R, Zhang Y. The long non-coding RNA MALAT1 interacted with miR-218 modulates choriocarcinoma growth by targeting Fbxw8. *Biomed Pharmacother* 97: 543–550, 2018. doi:10.1016/j.biopha.2017.10.083.
  29. Shih IM. Gestational trophoblastic neoplasia—pathogenesis and potential therapeutic targets. *Lancet Oncol* 8: 642–650, 2007. doi:10.1016/S1470-2045(07)70204-8.
  30. Takahashi M, Okimura Y, Iguchi G, Nishizawa H, Yamamoto M, Suda K, Kitazawa R, Fujimoto W, Takahashi K, Zolotaryov FN, Hong KS, Kiyonari H, Abe T, Kaji H, Kitazawa S, Kasuga M, Chihara K, Takahashi Y. Chemerin regulates  $\beta$ -cell function in mice. *Sci Rep* 1: 123, 2011. doi:10.1038/srep00123.
  31. Traboulsi W, Sergeant F, Boufettal H, Brouillet S, Slim R, Hoffmann P, Benlahfid M, Zhou QY, Balboni G, Onnis V, Bolze PA, Salomon A, Sauthier P, Mallet F, Aboussaouira T, Feige JJ, Benharouga M, Alfaidy N. Antagonism of EG-VEGF receptors as targeted therapy for choriocarcinoma progression *in vitro* and *in vivo*. *Clin Cancer Res* 23: 7130–7140, 2017. doi:10.1158/1078-0432.CCR-17-0811.
  32. Tuncer ZS, Vegh GL, Fulop V, Genest DR, Mok SC, Berkowitz RS. Expression of epidermal growth factor receptor-related family products in gestational trophoblastic diseases and normal placenta and its relationship with development of postmolar tumor. *Gynecol Oncol* 77: 389–393, 2000. doi:10.1006/gyno.2000.5777.
  33. Wagener J, Yang W, Kazuschke K, Winterhager E, Gellhaus A. CCN3 regulates proliferation and migration properties in Jeg3 trophoblast cells via ERK1/2, Akt and Notch signalling. *Mol Hum Reprod* 19: 237–249, 2013. doi:10.1093/molehr/gas061.
  34. Xie Y, Cui D, Sui L, Xu Y, Zhang N, Ma Y, Li Y, Kong Y. Induction of forkhead box M1 (FoxM1) by EGF through ERK signaling pathway promotes trophoblast cell invasion. *Cell Tissue Res* 362: 421–430, 2015. doi:10.1007/s00441-015-2211-y.
  35. Xue WC, Chan KY, Feng HC, Chiu PM, Ngan HY, Tsao SW, Cheung AN. Promoter hypermethylation of multiple genes in hydatidiform mole and choriocarcinoma. *J Mol Diagn* 6: 326–334, 2004. doi:10.1016/S1525-1578(10)60528-4.
  36. Yang X, Quan X, Lan Y, Ye J, Wei Q, Yin X, Fan F, Xing H. Serum chemerin level during the first trimester of pregnancy and the risk of gestational diabetes mellitus. *Gynecol Endocrinol* 33: 770–773, 2017. doi:10.1080/09513590.2017.1320382.
  37. Yang YL, Ren LR, Sun LF, Huang C, Xiao TX, Wang BB, Chen J, Zabel BA, Ren P, Zhang JV. The role of GPR1 signaling in mice corpus luteum. *J Endocrinol* 230: 55–65, 2016. doi:10.1530/JOE-15-0521.
  38. Zabel BA, Nakae S, Zúñiga L, Kim JY, Ohyama T, Alt C, Pan J, Suto H, Soler D, Allen SJ, Handel TM, Song CH, Galli SJ, Butcher EC. Mast cell-expressed orphan receptor CCR2 binds chemerin and is required for optimal induction of IgE-mediated passive cutaneous anaphylaxis. *J Exp Med* 205: 2207–2220, 2008. doi:10.1084/jem.20080300.
  39. Zheng C, Chen D, Zhang Y, Bai Y, Huang S, Zheng D, Liang W, She S, Peng X, Wang P, Mo X, Song Q, Lv P, Huang J, Ye RD, Wang Y. FAM19A1 is a new ligand for GPR1 that modulates neural stem-cell proliferation and differentiation. *FASEB J* 32: 5874–5890, 2018. doi:10.1096/fj.201800020RRR.